Electronic Journal of Biotechnology 52 (2021) 59–66

Contents lists available at ScienceDirect

Electronic Journal of Biotechnology

journal homepage:

Research Article

CRISPR-mediated base editing in mice using cytosine deaminase base editor 4

Salah Adlat [a,1], Farooq Hayel [a,1], Ping Yang [a], Yang Chen [a], Zin Mar Oo [a], May Zun Zaw Myint [a], Rajiv Kumar Sah [a], Noor Bahadar [a], Mahmoud Al-Azab [c], Fatoumata Binta Bah [a], Yaowu Zheng [a,b,d,*], Xuechao Feng [a,b,*]

[a] Transgenic Research Center, School of Life Sciences, Northeast Normal University, Changchun, Jilin 130024, China
[b] Key Laboratory of Molecular Epigenetics of Ministry of Education, School of Life Sciences, Northeast Normal University, Changchun, Jilin 130024, China
[c] Department of Immunology, Guangzhou Institute of Pediatrics, Guangzhou Women and Children's Medical Centre, Guangzhou Medical University, Guangzhou 510623, China
[d] Cardiovascular Research Institute, University of California, San Francisco, CA 94158, United States

ARTICLE INFO

Article history:
Received 10 November 2020
Accepted 28 April 2021
Available online 7 May 2021

Keywords:
Base editor 4
CRISPR-Cas9
Cytosine base editing
Cytosine Deaminase
Mouse model
Single-base substitution

ABSTRACT

Background: Many human genetic diseases arise from point mutations. These genetic diseases can theoretically be corrected through gene therapy. However, gene therapy in clinical application is still far from mature. Nearly half of the pathogenic single-nucleotide polymorphisms (SNPs) are caused by G:C>A:T or T:A>C:G base changes and the ideal approaches to correct these mutations are base editing. These CRISPR-Cas9-mediated base editing does not leave any footprint in genome and does not require donor DNA sequences for homologous recombination. These base editing methods have been successfully applied to cultured mammalian cells with high precision and efficiency, but BE4 has not been confirmed in mice. Animal models are important for dissecting pathogenic mechanism of human genetic diseases and testing of base correction efficacy in vivo. Cytidine base editor BE4 is a newly developed version of cytidine base editing system that converts cytidine (C) to uridine (U).

Results: In this study, BE4 system was tested in cells to inactivate GFP gene and in mice to introduce single-base substitution that would lead to a stop codon in tyrosinase gene. High percentage albino coat-colored mice were obtained from black coat-colored donor zygotes after pronuclei microinjection. Sequencing results showed that expected base changes were obtained with high precision and efficiency (56.25%). There are no off-targeting events identified in predicted potential off-target sites.

Conclusions: Results confirm BE4 system can work in vivo with high precision and efficacy, and has great potentials in clinic to repair human genetic mutations.

How to cite: Adlat S, Hayel F, Yang P, et al. CRISPR-mediated base editing in mice using cytosine deaminase base editor 4. Electron J Biotechnol 2021;52. https://doi.org/10.1016/j.ejbt.2021.04.010

1. Introduction

Point mutations are the most common causes in human genetic diseases and nearly 50% of disease-associated mutations are C>T and G>A substitutions [1,2,3]. Animal modeling of human genetic diseases are valuable in the study of pathogenic mechanism, testing of drug efficacy and proof of gene therapy reliability. CRISPR-Cas9 system is an adaptive immune system in bacteria that protects its genome from invading viruses [4,5]. CRISPR-Cas9 system has been successfully applied to genetic engineering in variety of cells and organisms. Targeted insertion and mutation usually require homologous recombination that is typically accomplished through cultured embryonic stem cells (ES cells), selection for positive clones and ES cell/blastocyst injection. This process is time-consuming and costly. CRISPR-Cas9 system has been applied to targeted gene engineering but efficiency of targeted insertion and base editing in vivo has been very low [6]. Homology-directed repair (HDR) with CRISPR-Cas9 system requires DNA double-strand breaks (DSBs) at the target and a DNA template with homologous arms [6,7,8,9]. Cells respond to DSBs and repair them often with nonhomologous end joining (NHEJ) that may introduce insertions or deletions (Indel formation) and lead to disruption of the

Peer review under responsibility of Pontificia Universidad Católica de Valparaíso
* Corresponding authors.
E-mail addresses: zhengyw442@nenu.edu.cn (Y. Zheng), fengxc997@nenu.edu.cn (X. Feng).
[1] These authors contributed equally.

https://doi.org/10.1016/j.ejbt.2021.04.010
0717-3458/

corresponding genes [10,11]. DSBs repair pathway by NHEJ lowers the efficiency of HDR as NHEJ is active during all stages of the cell cycle whereas HDR is only active during S and G2 phase. In addition, HDR in cultured cells often requires selection marker to remove the untransfected cells and to enrich the recombination events. This is not applicable to in vivo base editing that would not allow any selection makers. Therefore, higher in vivo editing efficiency is required. Base editing does not generate DSBs and reduces the possibility of indels. David Liu's lab has developed many versions of CRISPR-based base editing systems with improving accuracy and efficacy that eventually permit precise and efficient base change in cultured cells.

CRISPR-Cas9-based cytidine base editors (CBEs) have recently been developed to generate precise base changes from cytidine to thymidine with high efficiency [1,12,13,14]. CBE system consists of a CRISPR-Cas9-derived DNA-binding module, a cytidine deaminase and uracil glycosylase inhibitor (UGI). CBEs are able to introduce nucleotide substitutions of C>T [15,16,17] and G>A [18] without DSBs. It has been demonstrated successful in various cells and some organisms [16].

Base editing systems have gone through various stages of improvement to broaden their applicability in single nucleotide editing in cell lines and has been tested in various animals and plants [19,20,21,22,23]. The fourth generation of base editor (BE4) is one of the most advanced systems in base editing with high precision and efficiency in cultured mammalian cells. BE4 has a cytidine deaminase (rAPOBEC1) with two copies of UGI that are directly fused to C terminus of Cas9 nickase (Cas9n), a Cas9 mutant with a D10A amino acid substitution, through a 32 amino acid linker (Fig. 1A). BE4 enables direct conversion of cytidine (C) to uridine (U) in chosen target [11]. In the study, we have experimentally tested genes including Dip2a and Dip2c in cell culture that are highly expressed in central neuron system and known to be associated with autism and cancers [24,25] and Tyr gene that determines the coat color in mice. We confirmed that BE4 system is able to perform a multiplexed base editing with high precision and efficiency in mice. BE4 system shows great potentials in modeling human genetic diseases and for gene therapy.

2. Materials and methods

2.1. Animals

All mice and experimental protocols used in this project have been approved by Institutional Animal Care and Use Committee for Animal Experimental Ethics Committee of Northeast Normal University (NENU/IACUC, AP2018011) and carried out in accordance with recommendations in Guide for Care and Use of Laboratory Animals of National Institutes of Health as well. Mice were bred and maintained under specific pathogen-free condition in animal facility with controlled temperature at 21 ± 1°C, 30–60% humidity, 12:12 light/dark cycles and free access to food and water.

2.2. Reagents

Chemicals and reagents. Fetal bovine serum (FBS) was purchased from Hangzhou Sijiqing Biological Engineering Material, Co., Ltd. (Beijing, China). Dulbecco's modified Eagle's medium (DMEM) was obtained from Gibco (Thermo Fisher Scientific, Inc., Waltham, MA, USA). Opti-Mem medium, Lipofectamine, dimethyl sulfoxide (DMSO) were purchased from Sigma-Aldrich (Merck KGaA, Darmstadt, Germany). Dip2a and Dip2c antibodies were purchased from Novus and Signalway Antibody, Inc. (USA).

2.3. Plasmid construction and sgRNA design

Cas9 coding region of pX330 plasmid (Gifted from Dr. Feng Zhang, Addgene accession no. 42230) was replaced with EGFP cDNA (Fig. S1 A). EGFP sequence was PCR amplified from pEGFP-N1 (Clontech cat# 6059-1) (Fig. S1 B) using following primers: EGFP-F: 5′-GGCCACCGGTGATCCACCGGTCGCCACCAT-3′ (20b p) and EGFP-R: 5′-GGCCGAATTCTTACTTGTACAGCTCGTCCATG-3′ (22 bp) with AgeI site at 5′-end and EcoRI site at 3′-end (AgeI and EcoRI are shown by underline). PCR was performed at 94°C for 4 min, 24 cycles of 94°C for 30 s, 56°C for 30 s, 72°C for 1 min and 72°C for 10 min. EGFP PCR products were digested with AgeI and EcoRI (NEB) and inserted into AgeI and EcoRI sites of pX330. Resultant pX330-sgRNA-EGFP plasmid (Fig. S1 A) was confirmed by sequencing. Oligos coding for sgRNA targets were synthesized by Genewiz (Beijing, China), annealed at 95°C for 5 min and ramped down to 25°C (−5°C/min) and then subcloned into BbsI sites of pX330-sgRNA-EGFP. BE4 plasmid (Fig. 1A) was gifted from David Liu lab (Addgene access no. 100802). The sgRNAs were designed using online platform https://benchling.com/ and all sgRNAs oligos are listed in Table S1.

2.4. Cell culture and EGFP stable expression

Human embryonic kidney (HEK293) cells were from American Type Culture Collection (ATCC CRL-1573, Manassas, USA) and cultured in Dulbecco's modified Eagle's Medium (DMEM, Sigma) supplemented with fetal bovine serum (10%) and penicillin/streptomycin (Gibco, Life Technologies). Cells were maintained at 37°C and 5% CO2 in a humidified incubator. To stably express EGFP in HEK293, cells were seeded in 12-well plates with 1 ml of DMEM. When cells reached 60–80% confluency, medium was replaced with Opti-MEM (Gibco, Life Technologies). Then plasmids were transfected into the cells using Lipofectamine 2000 (Invitrogen) according to the manufacturer's protocol. One μg of pEGFP-N1 was transfected with 2 μL Lipofectamine 2000. Medium was replaced with fresh DMEM medium with serum 6 h after transfection. 48 h later, cells were treated with G418 (500 μg/mL, Sigma) for 15 d with medium changed every 3 d. Colonies were picked into 96 wells and expanded into 6-well plates before genomic DNA extraction, PCR amplification, and sequencing. Base editing frequencies were calculated by dividing the number of mutants by the total number of sequencing.

2.5. Plasmid transfection

SgRNA oligos (Table S1) were annealed and cloned into pX330-sgRNA-EGFP plasmid. HEK293 and B160F10 cells were transfected according to the manufacturer's protocols (Invitrogen, Cat. No. 11668-027). In brief, HEK293 and murine B16-F10 cells were seeded on 12-well plates in 1 ml of DMEM. When cells reached 60–80% confluency, medium was changed to Opti-MEM. Cells were then transfected with Lipofectamine 2000 (Invitrogen) according to the manufacturer's protocol. One μg pX330-sgRNA-EGFP and 2 μg BE4 plasmids were mixed with 2 μL Lipofectamine 2000. Six hours later, medium was replaced with fresh DMEM. Cells were then subjected to G418 treatment as described above.

2.6. Oocyte/DNA microinjection and oviduct transfer

Six-week old F1 female mice (B6D2F1) were obtained from mating of C57BL/6 and DBA2. Mice were superovulated with 10 IU of pregnant mare's serum gonadotropin (Ningbo Hormone Products CO., Ltd, Ningbo, Zhengjiang, China) and followed by 5 IU of human chorionic gonadotropin (Ningbo Hormone Products CO., Ltd, Ningbo, Zhengjiang, China) 48 h later. Superovulated

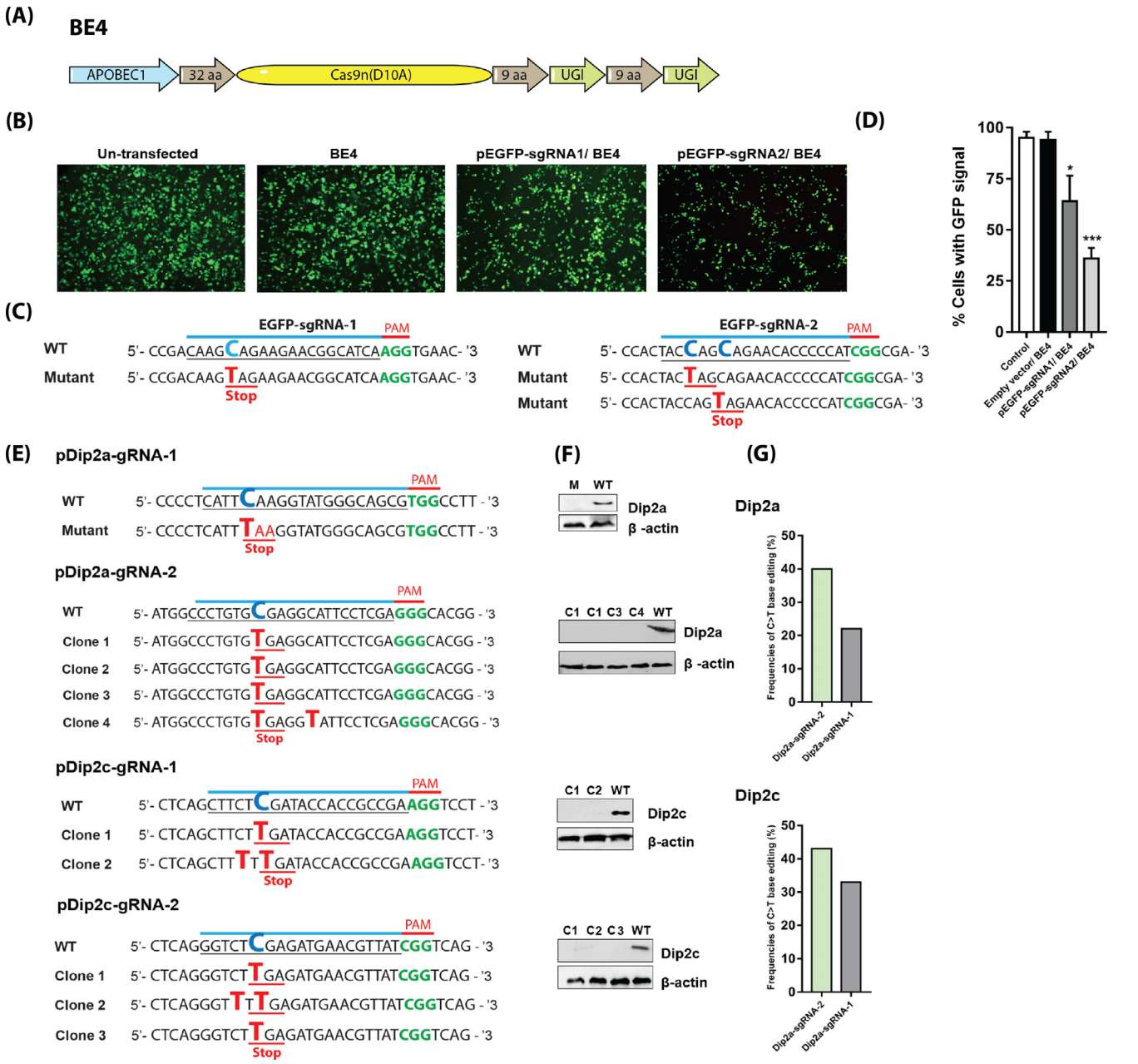

Fig. 1. Evaluating of BE4 activity in cells. (A) Architecture of cytosine base editor 4 (BE4), contains Cas9n fused to uracil glycosylase inhibitor domains (UGI) and cytidine deaminase. (B) Fluorescent imaging of transfected HEK293 cell stably expressing EGFP. Scale bar, 100 μm. (C) Base change in EGFP shown by sequencing. (D) Percentage of cells with GFP signal in B (E) Premature stop codon targeting of Dip2a and Dip2c genes in B16 cells. Protospacer Adjacent Motif (PAM) sequences labeled in green, wild type base in blue, mutated base in red and stop codon underlined. (F) Western blot analysis. β-actin served as a loading control. (G) Efficiency of C>T base editing. P-value was determined by t-test. $^{*}P < 0.05$, $^{***}P < 0.001$.

B6D2F1 females were crossed with B6D2F1 males. Fertilized eggs at pronucleus stage were collected in M2 medium. Mixtures of pTyr-gRNAs (2.35 ng/μl) and BE4 plasmids (2.64 ng/μl) were injected into the nucleus in a droplet of M2 medium using inverted microscope equipped with a pair of micromanipulators (Olympus, Tokyo, Japan). Then the injected embryos were incubated in M16 culture medium at 37°C, 6% CO2 overnight, followed by transfer into the oviduct of a recipient mother at two-cell stage.

2.7. Genomic DNA extraction and genotyping

Genomic DNA was extracted from mouse tail tips using G-NTK lysis buffer [26] and proteinase K (1 mg/ml) (Beijing Solarbio Science & Technology Co., Ltd., Beijing, China) at 55°C overnight. Proteinase K was deactivated at 95°C for 15 min and PCR was performed in 25 μl reaction volume with diluted tail DNA and genotyping primers (Table S2). PCR master mix was as follows: 1.2 μl of each primer (10 μM), 16.4 μl of ddH2O, 1.5 μl of 25 mM MgCl2, 2.5 μl of 10X PCR buffer, 0.5 μl of 10 mM dNTP Mix and 0.25 μl of Taq DNA Polymerase. The PCR conditions were as follows: 95°C for 5 min, 32 cycles of 95°C 30 s, 58°C 30 s and 72°C 30 s, and 72°C 10 min using PCR machine by Bio-Rad, Hercules, CA, USA.

2.8. RNA extraction

One ml RNAiso plus reagent (Takara, Dalian, China) was added to cells on 100 mm Petri dish. Cell lysates were collected and incubated at room temperature for 5 min. Cells were then centrifuged

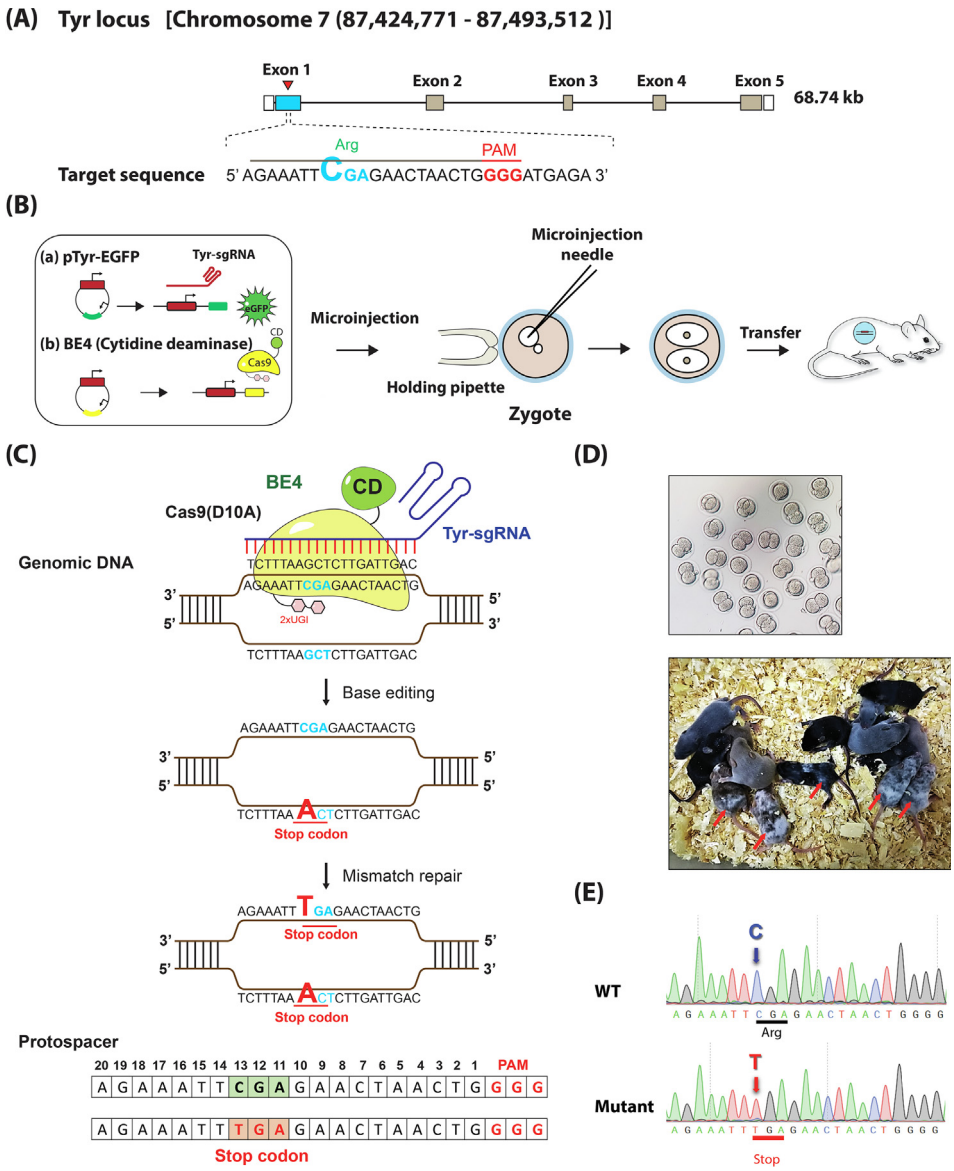

Fig. 2. BE4 mediated C>T base editing in mice. (A) Schematic of sgRNA design at Tyr locus. (B) Working model of base editing in mice. (C) Schematic depiction of BE4 base editing. The architecture of BE4 is containing Cas9 nickase fused to cytidine deaminase and two copies of uracil glycosylase inhibitor domains (2xUGI) for additional product purity. (D) Coat color of 8 day old Tyr mutant founders with mosaic pigmentation. (E) Chromatograms of WT and mutant sequences showing C>T substitution.

at 13,500× *g* for 5 min at 4°C. A 200 μL of CHCl3 was added, followed by 30 s mixing and 5 min incubation at RT, samples were centrifuged at 13500× *g* for 15 min at 4°C to separate RNA into aqueous phase. Aqueous phase (about 600 μl) was transferred to a new tube and RNA was precipitated with 750 μL of absolute isopropanol at RT for 10 min and then centrifuged at 13,500× *g* for 10 min at 4°C. Precipitate was washed with 1 mL 70% ethanol, followed by centrifugation at 13,500× *g* for 5 min at 4°C. RNA pellet was resuspended in 50 μL of DEPC-treated water. RNA concentrations were determined using NanoDrop 2000 (Thermo Fisher Scientific, USA). RNA integrity was checked on 0.8% agarose gel.

2.9. Quantitative real time PCR (qPCR)

One μg of total RNA was reverse-transcribed into first-strand complementary DNA (cDNA) with Prime Script RT Reagent Kit (Perfect Real Time, TaKaRa, Dalian, China) according to the manufacturer's instructions. Real-time PCR was performed with 50 ng of cDNA using One-Step SYBR PrimeScriptTM RT-PCR kit (Takara, Dalian, China). All reactions were performed in triplicate. All primers were initially evaluated for efficiency using relative standard curve and electrophoresis on gel. Primer sequences are listed in Table S3.

2.10. Mutation screening by sequencing

Purified PCR products were extracted using gel extraction kit (Qiagen, Germany) and cloned into pMD18-T plasmid (TaKaRa, Dalian, China). Positive clones were sequenced in two directions utilizing M13 forward and reverse primers. Mutations were identified by alignment to wild-type sequences.

2.11. Western blot

Total proteins were extracted using RIPA buffer (0.5% Nonidet P-40, 0.1% sodium deoxycholate, 150 mM NaCl, 50 mM Tris-Cl, pH 7.5 and 1x protease inhibitor cocktail). Cell lysates were subjected to high-speed centrifugation at 12,000× *g* for 15 min at

4°C. Protein concentrations were measured using Coomassie (Bradford) protein assay kit. Total soluble proteins were then separated on 10% SDS-PAGE and transferred into polyvinylidene difluoride membrane (Millipore, Billerica, MA). Membrane was blocked with 5% nonfat dry milk for 1 h followed by incubation with diluted the primary antibodies (β-actin, 1:2000, Signalway antibody; Dip2a, 1:500, Novus; Dip2c, 1:1000, Abcam) for overnight at 4°C. Then the membrane was washed in TBST for three times, 5 min each and then incubated with secondary antibody (anti-rabbit horseradish peroxidase conjugate, 1:5000; anti-mouse horseradish peroxidase conjugate, 1:5000; Transgene) for 30 min, followed by washing three times with TBST. Signals were detected using enhanced chemiluminescence Amersham™ ECL™ (GE Healthcare, USA) reagents. β-actin protein served as a loading control.

2.12. Off-target detection

Eight potential off-target sites (POTs) were identified according to an online design tool (https://benchling.com/). Selected POTs (Table 2) were amplified by PCR and sequenced. Sequences were compared with wild-type. All primers used for off-target assay are listed in Table 3.

2.13. Statistical analysis

Statistical analyses and graphics were performed with GraphPad Prism 5.01 (GraphPad Software Inc.) and SPSS software version 25.0 (IBM Inc., New York, USA). Parametric unpaired Student's t test was used to assess difference between the groups. P-values were two-sided; a *P*-value <0.05 was considered statistically significant.

3. Results and discussion

3.1. Testing sgRNAs in HEK293 cells

To test whether BE4 system works in our hands, we first transfected HEK293 cells stably expressing EGFP with BE4 and pEGFP-sgRNAs plasmids to inactivate the GFP by generating STOP codon (Fig. 1A). HEK293 cells stably expressing EGFP were generated by transfection of plasmid pEGFP-N1. EGFP expression was checked under a fluorescence microscope. Result showed up to 90% of cells with fluorescence (Fig. 1B). Positive clones expressing EGFP (HEK293-EGFP) were selected using G418 (500 μg/mL). Two sgRNAs were designed to target EGFP gene (Fig. 1C, Table S1). The specificity score of both sgRNA-1 and sgRNA-2 were 75%, and 83%, respectively, based on software analysis (https://benchling.com/). HEK293-EGFP cells were co-transfected with BE4 and plasmids encoding sgRNAs (pEGFP-sgRNA1 and pEGFP-sgRNA2). Two days after transfection, EGFP fluorescence intensity was analyzed by fluorescence microscopy (Fig. 1B). Majority of cells transfected with pEGFP-sgRNA1 still express relatively high levels of EGFP (64%), while cells transfected with pEGFP-sgRNA2 exhibited weak signal with an intensity of 36%, indicating EGFP was knocked down more efficiently (Fig. 1B, D).

3.2. Knockout of Dip2a and Dip2c genes in tumor cells using BE4

Next, BE4 system was analyzed in murine tumor cell B16-F10 to inactivate the *Dip2a* and *Dip2c* genes by generating STOP codon. *Dip2a* and *Dip2c* genes were each targeted with two sgRNAs (Fig. 1E, Table S1). Base substitutions were screened by genomic PCR amplification, DNA sequencing and western blotting.

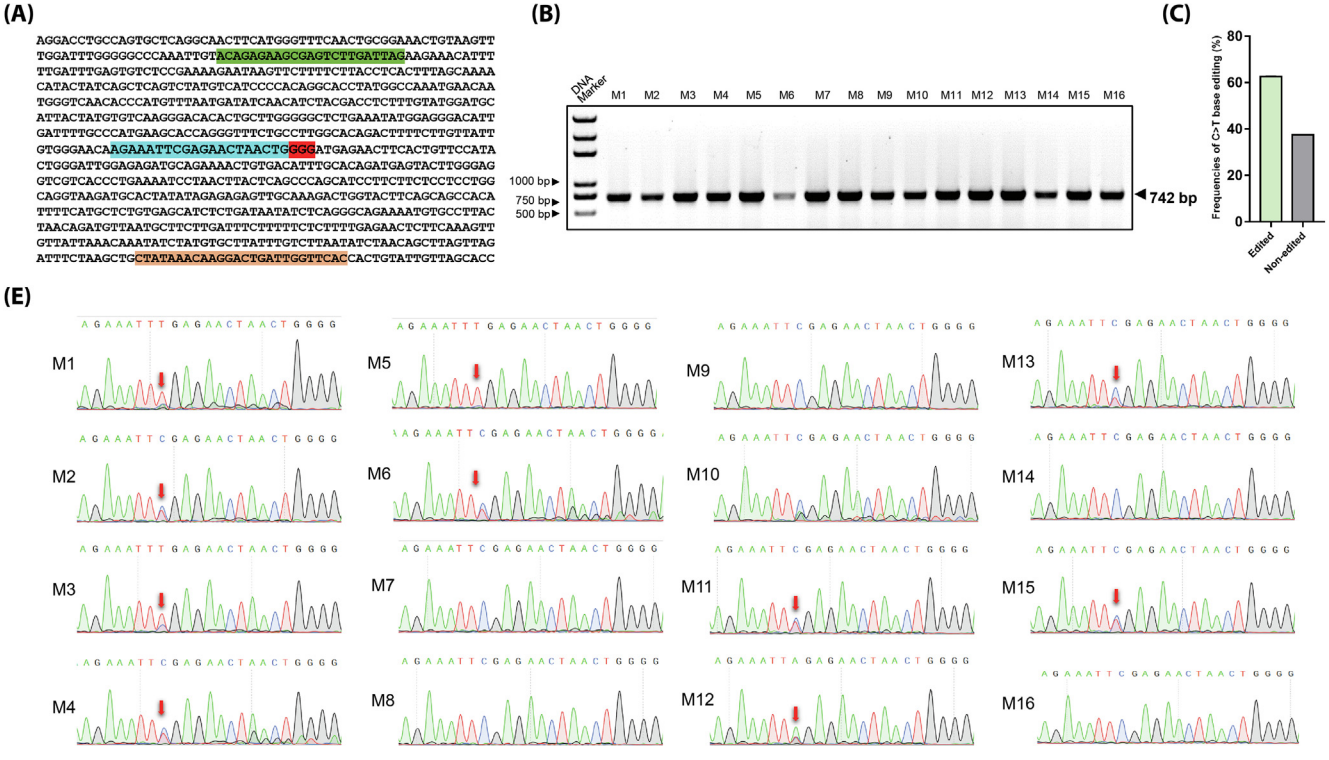

Fig. 3. Mice genotyping by genomic PCR and sequencing. (A) Sequences of Tyr gene target region in exon 1. SgRNA target sequence in blue and PCR primer sequences in green and orange. (B) Genomic PCR of target regions of founders 1–16 (F0). (C) Frequencies of C>T base editing. (E) Chromatograms showing sequencing signals of PCR amplified region. Red arrow shows the base change.

pDip2a-sgRNA-1 transfection results showed Q54Z mutation with an efficiency of 22% while pDip2c-sgRNA-1 showed mutations S72F and R73Z with a total efficiency of 33%. Knockout of Dip2a and Dip2c proteins using sgRNAs-1 are shown in Fig. 1 E–G, Fig. S2, Fig. S3. Similarly, pDip2a-sgRNA-2 and pDip2c-sgRNA-2 were transfected together with BE4 plasmid. Both pDip2a-sgRNA-2 and pDip2c-sgRNA-2 appeared to work more efficiently and induced 40% and 43% mutations at targeted sites, respectively (Fig. 1E–G, Fig. S4, Fig. S5). Expression of Dip2a and Dip2c genes from WT and mutated clones is shown in Fig. S6.

3.3. BE4 can induce C>T substitution in mice

To explore whether BE4 system can induce site-specific base conversion in mice, sgRNAs targeting exon 1 of Tyr locus were designed to inactivate tyrosinase gene (Fig. 2A). Target sequences were synthesized and cloned into pX330-sgRNA-EGFP to express both sgRNA and EGFP. pTyr-sgRNA (2.35 ng/μl) and BE4 plasmid (2.65 ng/μl) were co-injected into nucleus of B6/D2F1 mouse zygotes and transplanted into surrogate mothers at two-cell stage (Fig. 2B). pTyr-sgRNA/BE4 schematic depiction is shown in Fig. 2C. A total of 16 live pups were obtained (Fig. 2D, E). Mice were genotyped by genomic PCR using *Tyr* primers (): (Fig. 3A, B). PCR products were purified and sequenced to verify targeted point mutations (Fig. 3C, E). Results revealed that successful C>T transition with high efficiency was achieved. A total of 10 mice (62.5%) showed point mutations with C>T and C>A base conversion (Fig. 3D, 3E, Table 1). Mutations occurred at high efficiency at 13–15 bp upstream of PAM (Fig. S7). The editing frequencies of nonsense mutations in *Tyr* locus with expected amino-acid conversion from arginine to a stop codon (R224Z) were 56.25% (9 out of 16) (Fig. 3E, Table 1). These mutations resulted in a mosaic pigmentation phenotype. Some C>T substitution happened at two-cell stage or later after microinjection. Several founders exhibited obvious mosaicism (31%) phenomenon with a combination of non-mutant and mutant cells and a combination of homozygous and heterozygous cells. The mosaicism rate is lower than reported by Yen et al. [27] (68%), Sung et al. [28] (67%) and Zuo et al. [29] (77%). Founders 1#, 3# and #5 were homozygous for nonsense mutation at targeted site with a conversion rate of 18.75%. Founders 2#, #4, #6, #11, #13 and #15 showed heterozygous mutation with a frequency of 37.5%. Founders #7, #8, #9, #10, #14 and #16 were mostly wild-type alleles with a frequency of 37.5%. Meanwhile, C>A substitutions in founders #12 without amino acid

Table 1
Summary of the constructs, number of zygotes, and mutant mice obtained after BE4 and Tyr sgRNA microinjection.

Construct	Concentration	No. of injected zygotes	No. of transferred zygotes (%)[a]	No. of newborn mice (%)[a]	No. of living mice (%)[a]	Frequency substitution (%)[b]	Frequency of desired substitution (%)[b]	Error rate (%)[b]	Percentage of success (%)[b]
BE4	2.64 ng/μl	70	21 (30%)	16 (76.1%)	16 (76.1%)	10 (62.5%)	9 (56.25%)	1 (6.25%)	9 (56.25%)
Tyr-sgRNA	**2.35 ng/μl**								

[a] Calculated from the number of zygotes.
[b] Calculated from the number of living mice.

Table 2
List of potential off-target sites.

Off-target	Sequence (5′-3′)	PAM	Score	Mismatch numbers	Chromosome	Strand	Position
OT-1	GAGACTTGAGAACTAACTGT	TAG	1.514492754	3	chr2	1	116898149
OT-2	TTAGATTAGAGAACTAACTG	AGG	1.490585774	4	chr15	1	20069149
OT-3	TGAACTTTGCGAACTAACTG	AAG	1.45825	4	chr19	1	43539711
OT-4	AGAAATTGGAGAATTAACTG	GAG	0.996830986	2	chr7	1	74559357
OT-5	GGAGTTTCCAGAACTAACTG	GAG	0.92625	4	chr8	−1	46869033
OT-6	ATATCTTCAAGAACTAACTG	TGG	0.903189834	4	chr10	−1	103189990
OT-7	GGAATTTAGAGAACTAACTT	TAG	0.900340909	4	chr4	−1	24595654
OT8	AGAAATTGTAGAACTAACTC	AAG	0.853783	3	chr9	−1	100154656

Table 3
Primers list of potential off-target sites.

Off-target	Primer Sequences (5′-3′)	Amplicon (bp)	Annealing temperature (°C)
OT-1	Forward: 5′-CTCTACAGCTTGGCTCCTAAAC-3′ Reverse: 5′-GGTGGATTGCTCCAGAAAGA-3′	243	57
OT-2	Forward: 5′-GCTCAGCCTGCTCTCTTATAG-3′ Reverse: 5′-CAATATAGCCATGTATAGCCATGG-3′	420	57
OT-3	Forward: 5′-AAACACGTTCCTAGAGGAGAAAG-3′ Reverse: 5′-GTGTGTGATCAAAGAAGAGGATATTG-3′	428	57
OT-4	Forward: 5′-GCCTGACAATATCTGCCTAACA-3′ Reverse: 5′-GGGAGATCCAGAAAGCAAAGA-3′	318	57
OT-5	Forward: 5′-TTCTTTGTTTGCCTGGGTTTATC-3′ Reverse: 5′-TTATGGGTGCTTGACTCCTTAC-3′	495	57
OT-6	Forward: 5′-ATGCCGTCAATGCCAGTAAG-3′ Reverse: 5′-GCACTTGGGAGGTTAGAGTAGA-3′	398	57
OT-7	Forward: 5′-TGGGAATGTACCTCAGTGTTAG-3′ Reverse: 5′-CGGATGTCTCATATCCCTTCTC-3′	501	57
OT-8	Forward: 5′-CACAAACACCCTAGGATAGCTAAA-3′ Reverse: 5′-GGCCAAAGTCTCTGAAGGTAAA-3′	349	57

change was observed with a frequency of 6.25%. No indels were detected at target site (Fig. 3E). No off-target mutations were detected at potential off-target sites (Fig. S8). All results suggest that BE4 system is precise and efficient in introducing single point mutations into mouse genome, consistent with that single base substitution provides a secure approach to generate knockout animal models with minimum change of genome structure, mimicking most of the genetic diseases [23,30,31]. Lee et al. [32] have tested different versions of CBEs and find that BE4 system resulted in high frequency of anticipated C>T conversion but they tested the system only in embryos. In another study, Yuan et al. [33] used different versions of CBEs termed "AncBE4max and BE4-Gam". They showed success in generation of edited blastocyst and porcine fibroblasts. We achieved single-base substitution at target sites with efficiency of (56.25%) in mouse embryos. This study demonstrates the great values of BE4 editing in human disease modeling and correction of point mutations in future gene therapy.

4. Conclusion

In summary, this study has tested BE4 plasmid along with sgRNA expression plasmid in cell culture and applied to animal model by transgenic microinjection. We designed a precise base editing method to knockout tyrosinase gene and results in loss-of-pigmentation (Albinism). A high percentage of albino offspring was seen. C>T conversions have occurred exclusively within the approximate editing window of protospacers (positions ~ 4–8). BE-mediated STOP-codon generation disrupts gene function by converting C to T in coding sequences (CAG, CAA, CGA). Our study proves that BE4 system is highly efficient and precise, a powerful tool for generating disease models and correction of point mutations in future gene therapy.

Financial support

This work was funded supported by National Natural Science Foundation of China (81270953), the Natural Science Foundation of Jilin Province (20160101344JC) and Science and Technology Project of Jilin Provincial Education Department (JJKH20180023KJ). The funders had no roles in this study, including study design, data collection, data analysis or decision to publish or preparation of the manuscript.

Acknowledgements

We are grateful to Ms. Huiyan Wu for microinjection and managing mouse colony.

Conflict of interest

The authors declare that they have no competing interests.

Supplementary material

https://doi.org/10.1016/j.ejbt.2021.04.010.

References

[1] Burns MB, Temiz NA, Harris RS. Evidence for APOBEC3B mutagenesis in multiple human cancers. Nat Genet 2013;45(9):977–83. https://doi.org/10.1038/ng.2701.
[2] Gaudelli NM, Komor AC, Rees HA, et al. Programmable base editing of T to G C in genomic DNA without DNA cleavage. Nature 2017;551:464–71. https://doi.org/10.1038/nature24644. PMid: 29160308.
[3] Landrum MJ, Lee JM, Benson M, et al. ClinVar: Public archive of interpretations of clinically relevant variants. Nucleic Acids Res 2016;44:D862–8. https://doi.org/10.1093/nar/gkv1222. PMid: 26582918.
[4] Rath D, Amlinger L, Rath A, et al. The CRISPR-Cas immune system: Biology, mechanisms and applications. Biochimie 2015;117:119–28. https://doi.org/10.1016/j.biochi.2015.03.025. PMid: 25868999.
[5] Sontheimer EJ, Barrangou R. The bacterial origins of the CRISPR genome-editing revolution. Hum Gene Ther 2015;26(7):413–24. https://doi.org/10.1089/hum.2015.091. PMid: 26078042.
[6] Yin H, Xue W, Chen S, et al. Genome editing with Cas9 in adult mice corrects a disease mutation and phenotype. Nat Biotechnol 2014;32(6):551–3. https://doi.org/10.1038/nbt.2884. PMid: 24681508.
[7] Wu H, Liu Q, Shi H, et al. Engineering CRISPR/Cpf1 with tRNA promotes genome editing capability in mammalian systems. Cell Mol Life Sci 2018;75:3593–607. https://doi.org/10.1007/s00018-018-2810-3. PMid: 29637228.
[8] Yang Y, Wang K, Wu H, et al. Genetically humanized pigs exclusively expressing human insulin are generated through custom endonuclease-mediated seamless engineering. J Mol Cell Biol 2016;8:174–7. https://doi.org/10.1093/jmcb/mjw008. PMid: 26993040.
[9] Yang L, Guell M, Byrne S, et al. Optimization of scarless human stem cell genome editing. Nucleic Acids Res 2013;41:9049–61. https://doi.org/10.1093/nar/gkt555. PMid: 23907390.
[10] Davis AJ, Chen DJ. DNA double strand break repair via non-homologous end-joining. Transl Cancer Res 2013;2:130–43. https://doi.org/10.3978/j.issn.2218-676X.2013.04.02.
[11] Komor AC, Zhao KT, Packer MS, et al. Improved base excision repair inhibition and bacteriophage Mu Gam protein yields C:G-to-T: A base editors with higher efficiency and product purity. Sci Adv 2017;3. https://doi.org/10.1126/sciadv.aao4774. PMid: 28875174.
[12] Komor AC, Kim YB, Packer MS, et al. Programmable editing of a target base in genomic DNA without double-stranded DNA cleavage. Nature 2016;533:420–4. https://doi.org/10.1038/nature17946. PMid: 27096365.
[13] Nishida K, Arazoe T, Yachie N, et al. Targeted nucleotide editing using hybrid prokaryotic and vertebrate adaptive immune systems. Science 2016;353(6305):aaf8729. https://doi.org/10.1126/science.aaf8729. PMid: 27492474.
[14] Ma Y, Zhang J, Yin W, et al. Targeted AID-mediated mutagenesis (TAM) enables efficient genomic diversification in mammalian cells. Nat Methods 2016;13:1029–35. https://doi.org/10.1038/nmeth.4027. PMid: 27723754.
[15] Xie J, Ge W, Li N, et al. Efficient base editing for multiple genes and loci in pigs using base editors. Nat Commun 2019;10:2852. https://doi.org/10.1038/s41467-019-10421-8. PMid: 31253764.
[16] Kim D, Lim K, Kim ST, et al. Genome-wide target specificities of CRISPR RNA-guided programmable deaminases. Nat Biotechnol 2017;35:475–80. https://doi.org/10.1038/nbt.3852. PMid: 28398345.
[17] Kim K, Ryu SM, Kim ST, et al. Highly efficient RNA-guided base editing in mouse embryos. Nat Biotechnol 2017;35:435–7. https://doi.org/10.1038/nbt.3816. PMid: 28244995.
[18] Liu Z, Lu Z, Yang G, et al. Efficient generation of mouse models of human diseases via ABE- and BE-mediated base editing. Nat Commun 2018;9. https://doi.org/10.1038/s41467-018-04768-7. PMid: 29904106.
[19] Liu Z, Chen M, Chen S, et al. Highly efficient RNA-guided base editing in rabbit. Nat Commun 2018;9:2717. https://doi.org/10.1038/s41467-018-05232-2. PMid: 30006570.
[20] Zhang Y, Qin W, Lu X, et al. Programmable base editing of zebrafish genome using a modified CRISPR-Cas9 system. Nat Commun 2017;8:118. https://doi.org/10.1038/s41467-017-00175-6. PMid: 28740134.
[21] Zong Y, Wang Y, Li C, et al. Precise base editing in rice, wheat and maize with a Cas9-cytidine deaminase fusion. Nat Biotechnol 2017;35:438–40. https://doi.org/10.1038/nbt.3811. PMid: 28244994.
[22] Li G, Liu Y, Zeng Y, et al. Highly efficient and precise base editing in discarded human tripronuclear embryos. Protein Cell 2017;8:776–9. https://doi.org/10.1007/s13238-017-0458-7. PMid: 28825190.
[23] Yang G, Zhu T, Lu Z, et al. Generation of isogenic single and multiplex gene knockout mice by base editing-induced STOP. Sci Bull 2018;63:1101–7. https://doi.org/10.1016/j.scib.2018.07.002.
[24] Egger G, Roetzer KM, Noor A, et al. Identification of risk genes for autism spectrum disorder through copy number variation analysis in Austrian families. Neurogenetics 2014;15:117–27. https://doi.org/10.1007/s10048-014-0394-0. PMid: 24643514.
[25] Jiao X, Wood LD, Lindman M, et al. Somatic mutations in the notch, NF-KB, PIK3CA, and hedgehog pathways in human breast cancers. Genes Chromosom Cancer 2012;51:480–9. https://doi.org/10.1002/gcc.21935. PMid: 22302350.
[26] Malumbres M, Mangues R, Ferrer N, et al. Isolation of high molecular weight DNA for reliable genotyping of transgenic mice. Biotechniques 1997;22:1114–9. https://doi.org/10.2144/97226st03. PMid: 9187761.
[27] Yen ST, Zhang M, Deng JM, et al. Somatic mosaicism and allele complexity induced by CRISPR/Cas9 RNA injections in mouse zygotes. Dev Biol 2014;393:3–9. https://doi.org/10.1016/j.ydbio.2014.06.017. PMid: 24984260.
[28] Sung YH, Kim JM, Kim HT, et al. Highly efficient gene knockout in mice and zebrafish with RNA-guided endonucleases. Genome Res 2014;24:125–31. https://doi.org/10.1101/gr.163394.113. PMid: 24253447.
[29] Zuo E, Cai YJ, Li K, et al. One-step generation of complete gene knockout mice and monkeys by CRISPR/Cas9-mediated gene editing with multiple sgRNAs. Cell Res 2017;27:933–45. https://doi.org/10.1038/cr.2017.81. PMid: 28585534.

[30] Kuscu C, Parlak M, Tufan T, et al. CRISPR-STOP: Gene silencing through base-editing-induced nonsense mutations. Nat Methods 2017;14:710–2. https://doi.org/10.1038/nmeth.4327. PMid: 28581493.

[31] Billon P, Bryant EE, Joseph SA, et al. CRISPR-mediated base editing enables efficient disruption of eukaryotic genes through induction of STOP codons. Mol Cell 2017;67(1068–1079). https://doi.org/10.1016/j.molcel.2017.08.008. PMid: 28890334.

[32] Lee HK, Willi M, Miller SM, et al. Targeting fidelity of adenine and cytosine base editors in mouse embryos. Nat Commun 2018;9:4804. https://doi.org/10.1038/s41467-018-07322-7. PMid: 30442934.

[33] Yuan H, Yu T, Wang L, et al. Efficient base editing by RNA-guided cytidine base editors (CBEs) in pigs. Cell Mol Life Sci 2020;77:719–33. https://doi.org/10.1007/s00018-019-03205-2. PMid: 31302752.